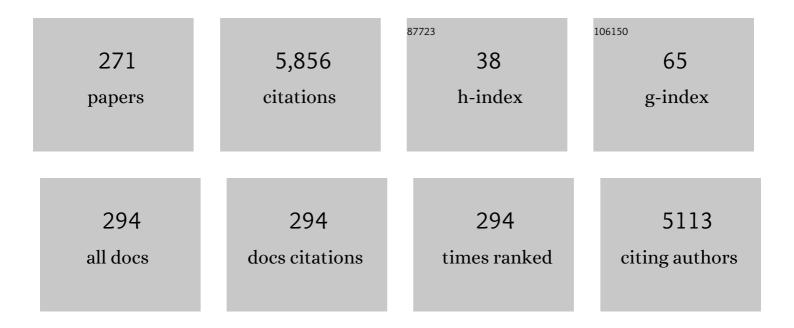
Guoyan Zheng

List of Publications by Year in descending order

Source: https://exaly.com/author-pdf/9179264/publications.pdf Version: 2024-02-01



#	Article	IF	CITATIONS
1	Tilt and Rotation Correction of Acetabular Version on Pelvic Radiographs. Clinical Orthopaedics and Related Research, 2005, &NA, 182-190.	0.7	264
2	What Are the Radiographic Reference Values for Acetabular Under- and Overcoverage?. Clinical Orthopaedics and Related Research, 2015, 473, 1234-1246.	0.7	250
3	Why rankings of biomedical image analysis competitions should be interpreted with care. Nature Communications, 2018, 9, 5217.	5.8	198
4	Crowd Counting with Deep Negative Correlation Learning. , 2018, , .		183
5	Evaluation of algorithms for Multi-Modality Whole Heart Segmentation: An open-access grand challenge. Medical Image Analysis, 2019, 58, 101537.	7.0	180
6	Standardized Assessment of Automatic Segmentation of White Matter Hyperintensities and Results of the WMH Segmentation Challenge. IEEE Transactions on Medical Imaging, 2019, 38, 2556-2568.	5.4	165
7	Radiographic analysis of femoroacetabular impingement with Hip ² norm—reliable and validated. Journal of Orthopaedic Research, 2008, 26, 1199-1205.	1.2	136
8	Benchmark on Automatic Six-Month-Old Infant Brain Segmentation Algorithms: The iSeg-2017 Challenge. IEEE Transactions on Medical Imaging, 2019, 38, 2219-2230.	5.4	136
9	Evaluation and Comparison of Anatomical Landmark Detection Methods for Cephalometric X-Ray Images: A Grand Challenge. IEEE Transactions on Medical Imaging, 2015, 34, 1890-1900.	5.4	135
10	A 2D/3D correspondence building method for reconstruction of a patient-specific 3D bone surface model using point distribution models and calibrated X-ray images. Medical Image Analysis, 2009, 13, 883-899.	7.0	132
11	Navigated open-wedge high tibial osteotomy: advantages and disadvantages compared to the conventional technique in a cadaver study. Knee Surgery, Sports Traumatology, Arthroscopy, 2006, 14, 917-921.	2.3	128
12	Computer aided high tibial open wedge osteotomy. Injury, 2004, 35, 68-78.	0.7	124
13	Which Radiographic Hip Parameters Do Not Have to Be Corrected for Pelvic Rotation and Tilt?. Clinical Orthopaedics and Related Research, 2015, 473, 1255-1266.	0.7	120
14	3D multi-scale FCN with random modality voxel dropout learning for Intervertebral Disc Localization and Segmentation from Multi-modality MR Images. Medical Image Analysis, 2018, 45, 41-54.	7.0	110
15	Statistical deformable bone models for robust 3D surface extrapolation from sparse data. Medical Image Analysis, 2007, 11, 99-109.	7.0	102
16	Computer-Assisted Orthopedic Surgery: Current State and Future Perspective. Frontiers in Surgery, 2015, 2, 66.	0.6	92
17	Fully Automatic Localization and Segmentation of 3D Vertebral Bodies from CT/MR Images via a Learning-Based Method. PLoS ONE, 2015, 10, e0143327.	1.1	86
18	Femoroacetabular Impingement Patients With Decreased Femoral Version Have Different Impingement Locations and Intra- and Extraarticular Anterior Subspine FAI on 3D-CT–Based Impingement Simulation: Implications for Hip Arthroscopy. American Journal of Sports Medicine, 2019, 47, 3120-3132.	1.9	85

#	Article	IF	CITATIONS
19	A Hybrid CT-Free Navigation System for Total Hip Arthroplasty. Computer Aided Surgery, 2002, 7, 129-145.	1.8	79
20	3D U-net with Multi-level Deep Supervision: Fully Automatic Segmentation of Proximal Femur in 3D MR Images. Lecture Notes in Computer Science, 2017, , 274-282.	1.0	75
21	Pelvic Tilt Is Minimally Changed by Total Hip Arthroplasty. Clinical Orthopaedics and Related Research, 2013, 471, 417-421.	0.7	74
22	Hip2Norm: An object-oriented cross-platform program for 3D analysis of hip joint morphology using 2D pelvic radiographs. Computer Methods and Programs in Biomedicine, 2007, 87, 36-45.	2.6	72
23	Novel adversarial semantic structure deep learning for MRI-guided attenuation correction in brain PET/MRI. European Journal of Nuclear Medicine and Molecular Imaging, 2019, 46, 2746-2759.	3.3	72
24	Multi-atlas pancreas segmentation: Atlas selection based on vessel structure. Medical Image Analysis, 2017, 39, 18-28.	7.0	70
25	Nonlinear Regression via Deep Negative Correlation Learning. IEEE Transactions on Pattern Analysis and Machine Intelligence, 2021, 43, 982-998.	9.7	68
26	Fully automatic segmentation of lumbar vertebrae from CT images using cascaded 3D fully convolutional networks. , 2018, , .		62
27	Evaluation and comparison of 3D intervertebral disc localization and segmentation methods for 3D T2 MR data: A grand challenge. Medical Image Analysis, 2017, 35, 327-344.	7.0	59
28	C-arm based navigation in total hip arthroplasty—background and clinical experience. Injury, 2004, 35, 90-95.	0.7	58
29	Navigated intraoperative analysis of lower limb alignment. Archives of Orthopaedic and Trauma Surgery, 2005, 125, 531-535.	1.3	57
30	Localization and Segmentation of 3D Intervertebral Discs in MR Images by Data Driven Estimation. IEEE Transactions on Medical Imaging, 2015, 34, 1719-1729.	5.4	57
31	Patient-Specific 3-D Magnetic Resonance Imaging–Based Dynamic Simulation of Hip Impingement and Range of Motion Can Replace 3-D Computed Tomography–Based Simulation for Patients With Femoroacetabular Impingement: Implications for Planning Open Hip Preservation Surgery and Hip Arthroscopy. American Journal of Sports Medicine, 2019, 47, 2966-2977.	1.9	54
32	Automatic X-ray landmark detection and shape segmentation via data-driven joint estimation of image displacements. Medical Image Analysis, 2014, 18, 487-499.	7.0	53
33	FACTS: Fully Automatic CT Segmentation of a Hip Joint. Annals of Biomedical Engineering, 2015, 43, 1247-1259.	1.3	49
34	Accurate and Robust Reconstruction of a Surface Model of the Proximal Femur From Sparse-Point Data and a Dense-Point Distribution Model for Surgical Navigation. IEEE Transactions on Biomedical Engineering, 2007, 54, 2109-2122.	2.5	45
35	Development of a balanced experimental–computational approach to understanding the mechanics of proximal femur fractures. Medical Engineering and Physics, 2014, 36, 793-799.	0.8	45
36	Reconstruction of Patient-Specific 3D Bone Surface from 2D Calibrated Fluoroscopic Images and Point Distribution Model. Lecture Notes in Computer Science, 2006, 9, 25-32.	1.0	43

#	Article	IF	CITATIONS
37	(i) Registration techniques for computer navigation. Orthopaedics and Trauma, 2007, 21, 170-179.	0.3	43
38	Automatic MRI-based Three-dimensional Models of Hip Cartilage Provide Improved Morphologic and Biochemical Analysis. Clinical Orthopaedics and Related Research, 2019, 477, 1036-1052.	0.7	43
39	MASCC: Multi-Atlas Segmentation Constrained Graph method for accurate segmentation of hip CT images. Medical Image Analysis, 2015, 26, 173-184.	7.0	40
40	Implementation, accuracy evaluation, and preliminary clinical trial of a CT-free navigation system for high tibial opening wedge osteotomy. Computer Aided Surgery, 2005, 10, 73-86.	1.8	38
41	Statistical shape model-based reconstruction of a scaled, patient-specific surface model of the pelvis from a single standard AP x-ray radiograph. Medical Physics, 2010, 37, 1424-1439.	1.6	38
42	3D reconstruction of a patientâ€specific surface model of the proximal femur from calibrated xâ€ray	1.6	37
43	OncoTREAT: a software assistant for cancer therapy monitoring. International Journal of Computer Assisted Radiology and Surgery, 2007, 1, 231-242.	1.7	35
44	Non-rigid free-form 2D–3D registration using a B-spline-based statistical deformation model. Pattern Recognition, 2017, 63, 689-699.	5.1	35
45	Is the acetabular cup orientation after total hip arthroplasty on a two dimension or three dimension model accurate?. International Orthopaedics, 2014, 38, 2009-2015.	0.9	34
46	Validation of statistical shape model based reconstruction of the proximal femur—A morphology study. Medical Engineering and Physics, 2010, 32, 638-644.	0.8	33
47	A hybrid CT-free navigation system for total hip arthroplasty. Computer Aided Surgery, 2002, 7, 129-145.	1.8	28
48	Biomechanical validation of computer assisted planning of periacetabular osteotomy: A preliminary study based on finite element analysis. Medical Engineering and Physics, 2015, 37, 1169-1173.	0.8	27
49	Spine-transformers: Vertebra labeling and segmentation in arbitrary field-of-view spine CTs via 3D transformers. Medical Image Analysis, 2022, 75, 102258.	7.0	27
50	Validation of a new method for determination of cup orientation in THA. Journal of Orthopaedic Research, 2009, 27, 1583-1588.	1.2	26
51	In Vivo Quantification of the Deformations of the Femoropopliteal Segment. Journal of Endovascular Therapy, 2017, 24, 27-34.	0.8	26
52	Bayesian VoxDRN: A Probabilistic Deep Voxelwise Dilated Residual Network for Whole Heart Segmentation from 3D MR Images. Lecture Notes in Computer Science, 2018, , 569-577.	1.0	26
53	Multi-stream 3D FCN with multi-scale deep supervision for multi-modality isointense infant brain MR image segmentation. , 2018, , .		26
54	Segmentation of the proximal femur in radial MR scans using a random forest classifier and deformable model registration. International Journal of Computer Assisted Radiology and Surgery, 2019, 14, 545-561.	1.7	26

#	Article	IF	CITATIONS
55	Computer Assisted Planning and Navigation of Periacetabular Osteotomy with Range of Motion Optimization. Lecture Notes in Computer Science, 2014, 17, 643-650.	1.0	25
56	Scaled, patient-specific 3D vertebral model reconstruction based on 2D lateral fluoroscopy. International Journal of Computer Assisted Radiology and Surgery, 2011, 6, 351-366.	1.7	24
57	A cost-effective surgical navigation solution for periacetabular osteotomy (PAO) surgery. International Journal of Computer Assisted Radiology and Surgery, 2016, 11, 271-280.	1.7	24
58	Holistic decomposition convolution for effective semantic segmentation of medical volume images. Medical Image Analysis, 2019, 57, 149-164.	7.0	24
59	Evaluation of an intensity-based algorithm for 2D/3D registration of natural knee videofluoroscopy data. Medical Engineering and Physics, 2020, 77, 107-113.	0.8	24
60	MRI-based 3D models of the hip joint enables radiation-free computer-assisted planning of periacetabular osteotomy for treatment of hip dysplasia using deep learning for automatic segmentation. European Journal of Radiology Open, 2021, 8, 100303.	0.7	24
61	X-ray image calibration and its application to clinical orthopedics. Medical Engineering and Physics, 2014, 36, 968-974.	0.8	23
62	Fully automatic reconstruction of personalized 3D volumes of the proximal femur from 2D X-ray images. International Journal of Computer Assisted Radiology and Surgery, 2016, 11, 1673-1685.	1.7	23
63	Fully automatic segmentation of paraspinal muscles from 3D torso CT images via multi-scale iterative random forest classifications. International Journal of Computer Assisted Radiology and Surgery, 2018, 13, 1697-1706.	1.7	23
64	Evaluation of Constant Thickness Cartilage Models vs. Patient Specific Cartilage Models for an Optimized Computer-Assisted Planning of Periacetabular Osteotomy. PLoS ONE, 2016, 11, e0146452.	1.1	23
65	Computer aided reduction and imaging. Injury, 2004, 35, 96-104.	0.7	22
66	HipMatch: An object-oriented cross-platform program for accurate determination of cup orientation using 2D–3D registration of single standard X-ray radiograph and a CT volume. Computer Methods and Programs in Biomedicine, 2009, 95, 236-248.	2.6	22
67	Validation of a statistical shape model-based 2D/3D reconstruction method for determination of cup orientation after THA. International Journal of Computer Assisted Radiology and Surgery, 2012, 7, 225-231.	1.7	22
68	Landmarkâ€based augmented reality system for paranasal and transnasal endoscopic surgeries. International Journal of Medical Robotics and Computer Assisted Surgery, 2009, 5, 415-422.	1.2	20
69	Effective incorporating spatial information in a mutual information based 3D–2D registration of a CT volume to X-ray images. Computerized Medical Imaging and Graphics, 2010, 34, 553-562.	3.5	20
70	Statistically Deformable 2D/3D Registration for Estimating Post-operative Cup Orientation from a Single Standard AP X-ray Radiograph. Annals of Biomedical Engineering, 2010, 38, 2910-2927.	1.3	20
71	An Integrated System for 3D Hip Joint Reconstruction from 2D X-rays: A Preliminary Validation Study. Annals of Biomedical Engineering, 2013, 41, 2077-2087.	1.3	20
72	Augmented marker tracking for peri-acetabular osteotomy surgery. International Journal of Computer Assisted Radiology and Surgery, 2018, 13, 291-304.	1.7	20

#	Article	IF	CITATIONS
73	Personalized X-Ray Reconstruction of the Proximal Femur via Intensity-Based Non-rigid 2D-3D Registration. Lecture Notes in Computer Science, 2011, 14, 598-606.	1.0	20
74	CyCMIS: Cycle-consistent Cross-domain Medical Image Segmentation via diverse image augmentation. Medical Image Analysis, 2022, 76, 102328.	7.0	20
75	Comparison of Computer Assisted Surgery with Conventional Technique for Treatment of Abaxial Distal Phalanx Fractures in Horses: An In Vitro Study. Veterinary Surgery, 2008, 37, 32-42.	0.5	19
76	Optimising conservative management of chronic low back pain: study protocol for a randomised controlled trial. Trials, 2017, 18, 184.	0.7	18
77	A fluoroscopy-based surgical navigation system for high tibial osteotomy. Technology and Health Care, 2005, 13, 469-483.	0.5	17
78	Gaussian mixture models based 2D–3D registration of bone shapes for orthopedic surgery planning. Medical and Biological Engineering and Computing, 2016, 54, 1727-1740.	1.6	17
79	Effect of Pelvic Tilt and Rotation on Cup Orientation in Both Supine and Standing Positions. Journal of Arthroplasty, 2018, 33, 1442-1448.	1.5	17
80	Surgically Relevant Morphological Parameters of Proximal Human Femur: A Statistical Analysis Based on 3D Reconstruction of CT Data. Orthopaedic Surgery, 2019, 11, 135-142.	0.7	17
81	Statistically Deformable 2D/3D Registration for Accurate Determination of Post-operative Cup Orientation from Single Standard X-ray Radiograph. Lecture Notes in Computer Science, 2009, 12, 820-827.	1.0	17
82	Comparison of 2.5D and 3D Quantification of Femoral Head Coverage in Normal Control Subjects and Patients with Hip Dysplasia. PLoS ONE, 2015, 10, e0143498.	1.1	17
83	A Robust and Accurate Two-Stage Approach for Automatic Recovery of Distal Locking Holes in Computer-Assisted Intramedullary Nailing of Femoral Shaft Fractures. IEEE Transactions on Medical Imaging, 2008, 27, 171-187.	5.4	16
84	Automatic extraction of proximal femur contours from calibrated X-ray images using 3D statistical models: an in vitro study. International Journal of Medical Robotics and Computer Assisted Surgery, 2009, 5, 213-222.	1.2	16
85	Development of an auditory implant manipulator for minimally invasive surgical insertion of implantable hearing devices. Journal of Laryngology and Otology, 2011, 125, 262-270.	0.4	16
86	Periacetabular osteotomy through the pararectus approach: technical feasibility and control of fragment mobility by a validated surgical navigation system in a cadaver experiment. International Orthopaedics, 2016, 40, 1389-1396.	0.9	16
87	Frameless Optical Computer-Aided Tracking of a Microscope for Otorhinology and Skull Base Surgery. JAMA Otolaryngology, 2001, 127, 1233.	1.5	15
88	Assessment of splineâ€based 2D–3D registration for imageâ€guided spine surgery. Minimally Invasive Therapy and Allied Technologies, 2006, 15, 193-199.	0.6	15
89	3D volumetric intensity reconsturction from 2D x-ray images using partial least squares regression. , 2013, , .		15
90	Use of a Dense Surface Point Distribution Model in a Three-Stage Anatomical Shape Reconstruction from Sparse Information for Computer Assisted Orthopaedic Surgery: A Preliminary Study. Lecture Notes in Computer Science, 2006, , 52-60.	1.0	15

#	Article	IF	CITATIONS
91	Automated Vertebra Identification from X-Ray Images. Lecture Notes in Computer Science, 2010, , 1-9.	1.0	15
92	Comparison of partial least squares regression and principal component regression for pelvic shape prediction. Journal of Biomechanics, 2013, 46, 197-199.	0.9	14
93	Statistical model-based segmentation of the proximal femur in digital antero-posterior (AP) pelvic radiographs. International Journal of Computer Assisted Radiology and Surgery, 2014, 9, 165-176.	1.7	14
94	Semantic Consistent Unsupervised Domain Adaptation for Cross-Modality Medical Image Segmentation. Lecture Notes in Computer Science, 2021, , 201-210.	1.0	14
95	Endoscope-based hybrid navigation system for minimally invasive ventral spine surgeries. Computer Aided Surgery, 2005, 10, 351-356.	1.8	13
96	Surface Reconstruction of Bone from X-ray Images and Point Distribution Model Incorporating a Novel Method for 2D-3D Correspondence. , 0, , .		13
97	A novel technology for 3D knee prosthesis planning and treatment evaluation using 2D X-ray radiographs: a clinical evaluation. International Journal of Computer Assisted Radiology and Surgery, 2018, 13, 1151-1158.	1.7	13
98	Unsupervised Reconstruction of a Patient-Specific Surface Model of a Proximal Femur from Calibrated Fluoroscopic Images. , 2007, 10, 834-841.		13
99	An Optimized Spline-Based Registration of a 3D CT to a Set of C-Arm Images. International Journal of Biomedical Imaging, 2006, 2006, 1-12.	3.0	12
100	Axial suspension test to assess pre-operative spinal flexibility in patients with adolescent idiopathic scoliosis. European Spine Journal, 2014, 23, 2619-2625.	1.0	12
101	Ruler Based Automatic C-Arm Image Stitching Without Overlapping Constraint. Journal of Digital Imaging, 2015, 28, 474-480.	1.6	12
102	Deep Learning-Based Automatic Segmentation of the Proximal Femur from MR Images. Advances in Experimental Medicine and Biology, 2018, 1093, 73-79.	0.8	12
103	Hybrid Generative Adversarial Networks for Deep MR to CT Synthesis Using Unpaired Data. Lecture Notes in Computer Science, 2019, , 759-767.	1.0	12
104	Computer assisted determination of acetabular cup orientation using 2D–3D image registration. International Journal of Computer Assisted Radiology and Surgery, 2010, 5, 437-447.	1.7	11
105	Precise Estimation of Postoperative Cup Alignment from Single Standard X-Ray Radiograph with Gonadal Shielding. , 2007, 10, 951-959.		11
106	A Novel 3D/2D Correspondence Building Method for Anatomy-Based Registration. Lecture Notes in Computer Science, 2006, , 75-83.	1.0	10
107	Calibration of C-arm for orthopedic interventions via statistical model-based distortion correction and robust phantom detection. , 2012, , .		10
108	Cup Implant Planning Based on 2-D/3-D Radiographic Pelvis Reconstruction—First Clinical Results. IEEE Transactions on Biomedical Engineering, 2015, 62, 2665-2673.	2.5	10

#	Article	IF	CITATIONS
109	Computer-Assisted Planning, Simulation, and Navigation System for Periacetabular Osteotomy. Advances in Experimental Medicine and Biology, 2018, 1093, 143-155.	0.8	10
110	How to Exploit Weaknesses in Biomedical Challenge Design and Organization. Lecture Notes in Computer Science, 2018, , 388-395.	1.0	10
111	A Projector-Based Augmented Reality Navigation System for Computer-Assisted Surgery. Sensors, 2021, 21, 2931.	2.1	10
112	Articulated Statistical Shape Model-Based 2D-3D Reconstruction of a Hip Joint. Lecture Notes in Computer Science, 2014, , 128-137.	1.0	10
113	Does the Rule of Thirds Adequately Detect Deficient and Excessive Acetabular Coverage?. Clinical Orthopaedics and Related Research, 2021, 479, 974-987.	0.7	10
114	Calibration of a surgical microscope with automated zoom lenses using an active optical tracker. International Journal of Medical Robotics and Computer Assisted Surgery, 2008, 4, 87-93.	1.2	9
115	3-D reconstruction of a surface model of the proximal femur from digital biplanar radiographs. , 2008, 2008, 66-9.		9
116	Effect of Stent Implantation on the Deformations of the Superficial Femoral Artery and Popliteal Artery: In Vivo Three-Dimensional Deformational Analysis from Two-Dimensional Radiographs. Journal of Vascular and Interventional Radiology, 2017, 28, 142-146.	0.2	9
117	Computer-Aided Orthopaedic Surgery: State-of-the-Art and Future Perspectives. Advances in Experimental Medicine and Biology, 2018, 1093, 1-20.	0.8	9
118	Automatic Extraction of Femur Contours from Calibrated X-Ray Images using Statistical Information. Journal of Multimedia, 2007, 2, .	0.3	9
119	Deep learning-based 2D/3D registration of an atlas to biplanar X-ray images. International Journal of Computer Assisted Radiology and Surgery, 2022, 17, 1333-1342.	1.7	9
120	Robust automatic detection and removal of fiducial projections in fluoroscopy images: An integrated solution. Medical Engineering and Physics, 2009, 31, 571-580.	0.8	8
121	An integrated approach for reconstructing a surface model of the proximal femur from sparse input data and a multi-resolution point distribution model: an in vitro study. International Journal of Computer Assisted Radiology and Surgery, 2010, 5, 99-107.	1.7	8
122	Statistical Shape and Deformation Models Based 2D–3D Reconstruction. , 2017, , 329-349.		8
123	Latent3DU-net: Multi-level Latent Shape Space Constrained 3D U-net for Automatic Segmentation of the Proximal Femur from Radial MRI of the Hip. Lecture Notes in Computer Science, 2018, , 188-196.	1.0	8
124	Effect of pelvic tilt and rotation on cup orientation in standing anteroposterior radiographs. HIP International, 2020, 30, 48-55.	0.9	8
125	Spine-Transformers: Vertebra Detection and Localization in Arbitrary Field-of-View Spine CT with Transformers. Lecture Notes in Computer Science, 2021, , 93-103.	1.0	8
126	3D Tiled Convolution for Effective Segmentation of Volumetric Medical Images. Lecture Notes in Computer Science, 2019, , 146-154.	1.0	8

#	Article	IF	CITATIONS
127	Entropy Guided Unsupervised Domain Adaptation for Cross-Center Hip Cartilage Segmentation from MRI. Lecture Notes in Computer Science, 2020, , 447-456.	1.0	8
128	3D Intervertebral Disc Localization and Segmentation from MR Images by Data-Driven Regression and Classification. Lecture Notes in Computer Science, 2014, , 50-58.	1.0	8
129	A CT-free, intra-operative planning and navigation system for minimally invasive anterior spinal surgery - an accuracy study. Computer Aided Surgery, 2007, 12, 233-241.	1.8	8
130	Landmark based augmented reality endoscope system for sinus and skull-base surgeries. , 2008, 2008, 74-7.		7
131	Automated Intervertebral Disc Detection from Low Resolution, Sparse MRI Images for the Planning of Scan Geometries. Lecture Notes in Computer Science, 2010, , 10-17.	1.0	7
132	Compensation of Sound Speed Deviations in 3-D B-Mode Ultrasound for Intraoperative Determination of the Anterior Pelvic Plane. IEEE Transactions on Information Technology in Biomedicine, 2012, 16, 88-97.	3.6	7
133	Automated Recognition of Erector Spinae Muscles and Their Skeletal Attachment Region via Deep Learning in Torso CT Images. Lecture Notes in Computer Science, 2019, , 1-10.	1.0	7
134	Editorial: Artificial Intelligence for Medical Image Analysis of Neuroimaging Data. Frontiers in Neuroscience, 2020, 14, 480.	1.4	7
135	Robust and Accurate Reconstruction of Patient-Specific 3D Surface Models from Sparse Point Sets: A Sequential Three-Stage Trimmed Optimization Approach. Lecture Notes in Computer Science, 2006, , 68-75.	1.0	7
136	Effective Incorporation of Spatial Information in a Mutual Information Based 3D-2D Registration of a CT Volume to X-Ray Images. Lecture Notes in Computer Science, 2008, 11, 922-929.	1.0	7
137	Determination of Pelvic Orientation from Ultrasound Images Using Patch-SSMs and a Hierarchical Speed of Sound Compensation Strategy. Lecture Notes in Computer Science, 2010, , 157-167.	1.0	7
138	Fully Automatic Segmentation of AP Pelvis X-rays via Random Forest Regression and Hierarchical Sparse Shape Composition. Lecture Notes in Computer Science, 2013, , 335-343.	1.0	7
139	Implementation, accuracy evaluation, and preliminary clinical trial of a CT-free navigation system for high tibial opening wedge osteotomy. Computer Aided Surgery, 2005, 10, 73-86.	1.8	7
140	Reconstruction of Patient-Specific 3D Bone Model from Biplanar X-Ray Images and Point Distribution Models. , 2006, , .		6
141	Automatic Extraction of Femur Contours from Calibrated Fluoroscopic Images. Proceedings IEEE Workshop on Applications of Computer Vision, 2007, , .	0.0	6
142	Fully automatic segmentation of AP pelvis X-rays via random forest regression with efficient feature selection and hierarchical sparse shape composition. Computer Vision and Image Understanding, 2014, 126, 1-10.	3.0	6
143	Patient-specific spinal stiffness in AIS: a preoperative and noninvasive method. European Spine Journal, 2015, 24, 249-255.	1.0	6
144	Fluoroscopy-based tracking of femoral kinematics with statistical shape models. International Journal of Computer Assisted Radiology and Surgery, 2016, 11, 757-765.	1.7	6

#	Article	IF	CITATIONS
145	Radiographic reconstruction of lower-extremity bone fragments: a first trial. International Journal of Computer Assisted Radiology and Surgery, 2016, 11, 2241-2251.	1.7	6
146	Proof of concept: hip joint damage occurs at the zone of femoroacetabular impingement (FAI) in an experimental FAI sheep model. Osteoarthritis and Cartilage, 2019, 27, 1075-1083.	0.6	6
147	Frequency-Supervised MR-to-CT Image Synthesis. Lecture Notes in Computer Science, 2021, , 3-13.	1.0	6
148	3D Model-based Reconstruction of the Proximal Femur from Low-dose Biplanar X-Ray Images. , 2011, , .		6
149	Automated Intervertebral Disc Segmentation Using Deep Convolutional Neural Networks. Lecture Notes in Computer Science, 2016, , 38-48.	1.0	6
150	Computer-assisted LISS plate osteosynthesis of proximal tibia fractures: Feasibility study and first clinical results. Computer Aided Surgery, 2005, 10, 141-149.	1.8	6
151	A fluoroscopy-based surgical navigation system for high tibial osteotomy. Technology and Health Care, 2005, 13, 469-83.	0.5	6
152	Minimal Invasive Spinal Surgery. International Journal of Computer Assisted Radiology and Surgery, 2006, 1, 189-200.	1.7	5
153	A Unifying MAP-MRF Framework for Deriving New Point Similarity Measures for Intensity-based 2D-3D Registration. , 2006, , .		5
154	Automated detection and segmentation of cylindrical fragments from calibrated C-arm images for long bone fracture reduction. Computer Methods and Programs in Biomedicine, 2007, 87, 1-11.	2.6	5
155	Calibration of X-ray radiographs and its feasible application for 2D/3D reconstruction of the proximal femur. , 2008, 2008, 470-3.		5
156	Assessing the Accuracy Factors in the Determination of Postoperative Acetabular Cup Orientation Using Hybrid 2D–3D Registration. Journal of Digital Imaging, 2010, 23, 769-779.	1.6	5
157	2D/3D reconstruction of a scaled lumbar vertebral model from a single fluoroscopic image. , 2010, 2010, 4395-8.		5
158	Clinical experience with computer navigation in revision total hip arthroplasty. Proceedings of the Institution of Mechanical Engineers, Part H: Journal of Engineering in Medicine, 2012, 226, 919-926.	1.0	5
159	Determination of pelvic orientation from sparse ultrasound data for THA operated in the lateral position. International Journal of Medical Robotics and Computer Assisted Surgery, 2012, 8, 107-113.	1.2	5
160	A multi-criteria decision support for optimal instrumentation in scoliosis spine surgery. Structural and Multidisciplinary Optimization, 2012, 45, 917-929.	1.7	5
161	Medical image computing in diagnosis and intervention of spinal diseases. Computerized Medical Imaging and Graphics, 2015, 45, 99-101.	3.5	5
162	Patient-Specific 3D Reconstruction of a Complete Lower Extremity from 2D X-rays. Lecture Notes in Computer Science, 2016, , 404-414.	1.0	5

#	Article	IF	CITATIONS
163	Multi-object Model-Based Multi-atlas Segmentation Constrained Grid Cut for Automatic Segmentation of Lumbar Vertebrae from CT Images. Advances in Experimental Medicine and Biology, 2018, 1093, 65-71.	0.8	5
164	DSMS-FCN: A Deeply Supervised Multi-scale Fully Convolutional Network for Automatic Segmentation of Intervertebral Disc in 3D MR Images. Lecture Notes in Computer Science, 2018, , 148-159.	1.0	5
165	Expectation Conditional Maximization-Based Deformable Shape Registration. Lecture Notes in Computer Science, 2013, , 548-555.	1.0	5
166	Endoscope-based hybrid navigation system for minimally invasive ventral spine surgeries. Computer Aided Surgery, 2005, 10, 351-356.	1.8	5
167	Handling Imbalanced Data: Uncertainty-Guided Virtual Adversarial Training With Batch Nuclear-Norm Optimization for Semi-Supervised Medical Image Classification. IEEE Journal of Biomedical and Health Informatics, 2022, 26, 2983-2994.	3.9	5
168	Image-Less THA Cup Navigation in Clinical Routine Setup: Individual Adjustments, Accuracy, Precision, and Robustness. Medicina (Lithuania), 2022, 58, 832.	0.8	5
169	Novel method for registering an endoscope in an operative setup. , 2005, 2005, 4349-52.		4
170	A novel parameter decomposition based optimization approach for automatic pose estimation of distal locking holes from single calibrated fluoroscopic image. Pattern Recognition Letters, 2009, 30, 838-847.	2.6	4
171	Personalized x-ray reconstruction of the proximal femur via a non-rigid 2D-3D registration. Proceedings of SPIE, 2015, , .	0.8	4
172	A complete-pelvis segmentation framework for image-free total hip arthroplasty (THA): methodology and clinical study. International Journal of Medical Robotics and Computer Assisted Surgery, 2015, 11, 166-180.	1.2	4
173	Augmented marker tracking for peri-acetabular osteotomy surgery. , 2017, 2017, 937-941.		4
174	A software program to measure the three-dimensional length of the spine from radiographic images: Validation and reliability assessment for adolescent idiopathic scoliosis. Computer Methods and Programs in Biomedicine, 2017, 138, 57-64.	2.6	4
175	Biomechanical Optimization-Based Planning of Periacetabular Osteotomy. Advances in Experimental Medicine and Biology, 2018, 1093, 157-168.	0.8	4
176	Multi-scale Fully Convolutional DenseNets for Automated Skin Lesion Segmentation in Dermoscopy Images. Lecture Notes in Computer Science, 2018, , 513-521.	1.0	4
177	A Deep Learning Approach to Horse Bone Segmentation from Digitally Reconstructed Radiographs. , 2019, , .		4
178	Fully Automatic Localization and Segmentation of Intervertebral Disc from 3D Multi-modality MR Images by Regression Forest and CNN. Lecture Notes in Computer Science, 2016, , 92-101.	1.0	4
179	Automatic Extraction of Proximal Femur Contours from Calibrated X-Ray Images Using 3D Statistical Models. Lecture Notes in Computer Science, 2008, , 421-429.	1.0	4
180	Statistical Deformable Model-Based Reconstruction of a Patient-Specific Surface Model from Single Standard X-ray Radiograph. Lecture Notes in Computer Science, 2009, , 672-679.	1.0	4

#	Article	IF	CITATIONS
181	Increased Combined Anteversion Is an Independent Predictor of Ischiofemoral Impingement in the Setting of Borderline Dysplasia With Coxa Profunda. Arthroscopy - Journal of Arthroscopic and Related Surgery, 2022, 38, 1519-1527.	1.3	4
182	Entropy and distance maps-guided segmentation of articular cartilage: data from the Osteoarthritis Initiative. International Journal of Computer Assisted Radiology and Surgery, 2022, 17, 553-560.	1.7	4
183	What Factors Are Associated With Postoperative Ischiofemoral Impingement After Bernese Periacetabular Osteotomy in Developmental Dysplasia of the Hip?. Clinical Orthopaedics and Related Research, 2022, Publish Ahead of Print, .	0.7	4
184	A robust and accurate approach for reconstruction of patient-specific 3D bone models from sparse point sets. , 2007, , .		3
185	Development of a miniature robot for hearing aid implantation. , 2009, , .		3
186	Automated detection of fiducial screws from CT/DVT volume data for image-guided ENT surgery. , 2010, 2010, 2325-8.		3
187	2D-3D regularized deformable b-spline registration: Application to the proximal femur. , 2015, , .		3
188	Constrained Statistical Modelling of Knee Flexion From Multi-Pose Magnetic Resonance Imaging. IEEE Transactions on Medical Imaging, 2016, 35, 1686-1695.	5.4	3
189	Application of Image Processing Techniques in Molecular Imaging of Cancer. Contrast Media and Molecular Imaging, 2017, 2017, 1-2.	0.4	3
190	Fully Automatic Planning of Total Shoulder Arthroplasty Without Segmentation: A Deep Learning Based Approach. Lecture Notes in Computer Science, 2019, , 22-34.	1.0	3
191	Evaluation of CTâ€MR image registration methodologies for 3D preoperative planning of forearm surgeries. Journal of Orthopaedic Research, 2020, 38, 1920-1930.	1.2	3
192	2D/3D Registration with a Statistical Deformation Model Prior Using Deep Learning. , 2021, , .		3
193	Automated 3D Lumbar Intervertebral Disc Segmentation from MRI Data Sets. Lecture Notes in Computational Vision and Biomechanics, 2016, , 25-40.	0.5	3
194	New orthopaedic implant management tool for computer-assisted planning, navigation, and simulation: From implant CAD files to a standardized XML-based implant database. Computer Aided Surgery, 2005, 10, 311-319.	1.8	3
195	Kernel Regularized Bone Surface Reconstruction from Partial Data Using Statistical Shape Model. , 2005, 2005, 6579-82.		2
196	Automated Detection and Segmentation of Diaphyseal Bone Fragments From Registered C-Arm Images for Long Bone Fracture Reduction. , 2005, 2005, 4361-4.		2
197	Integration of intraoperative imaging and surgical robotics to increase their acceptance. International Journal of Computer Assisted Radiology and Surgery, 2007, 1, 243-251.	1.7	2
198	Automatic extraction of femur contours from calibrated x-ray images: A Bayesian inference approach. , 2008, , .		2

#	Article	IF	CITATIONS
199	Reality-augmented virtual fluoroscopy for computer-assisted diaphyseal long bone fracture osteosynthesis: A novel technique and feasibility study results. Proceedings of the Institution of Mechanical Engineers, Part H: Journal of Engineering in Medicine, 2008, 222, 101-115.	1.0	2
200	Evaluation of 3D correspondence methods for building point distribution models of the kidney. , 2012, , .		2
201	Reconstruction of 3D Vertebral Models from a Single 2D Lateral Fluoroscopic Image. Lecture Notes in Computational Vision and Biomechanics, 2015, , 349-365.	0.5	2
202	A Cost-Effective Navigation System for Peri-acetabular Osteotomy Surgery. Lecture Notes in Computer Science, 2016, , 84-95.	1.0	2
203	Independent Evaluation of a Mechanical Hip Socket Navigation System in Total Hip Arthroplasty. Journal of Arthroplasty, 2016, 31, 658-661.	1.5	2
204	Fully Automatic Segmentation of Hip CT Images. Lecture Notes in Computational Vision and Biomechanics, 2016, , 91-110.	0.5	2
205	3X-Knee: A Novel Technology for 3D Preoperative Planning and Postoperative Evaluation of TKA Based on 2D X-Rays. Advances in Experimental Medicine and Biology, 2018, 1093, 93-103.	0.8	2
206	Atlas-Based 3D Intensity Volume Reconstruction from 2D Long Leg Standing X-Rays: Application to Hard and Soft Tissues in Lower Extremity. Advances in Experimental Medicine and Biology, 2018, 1093, 105-112.	0.8	2
207	EquiSim: An Open-Source Articulatable Statistical Model of the Equine Distal Limb. Frontiers in Veterinary Science, 2021, 8, 623318.	0.9	2
208	Automatic Localization of the Lumbar Vertebral Landmarks in CT Images with Context Features. Lecture Notes in Computer Science, 2018, , 59-71.	1.0	2
209	Automated Grading of Modic Changes Using CNNs – Improving the Performance with Mixup. Lecture Notes in Computer Science, 2019, , 41-52.	1.0	2
210	MCG-Net: End-to-End Fine-Grained Delineation and Diagnostic Classification of Cardiac Events From Magnetocardiographs. IEEE Journal of Biomedical and Health Informatics, 2022, 26, 1057-1067.	3.9	2
211	Computerized fluoroscopy with zero-dose image updates for minimally invasive femoral diaphyseal fracture reduction. , 2006, , .		1
212	Computer Assisted Orthopaedic Surgery. International Journal of Computer Assisted Radiology and Surgery, 2006, 1, 229-250.	1.7	1
213	A Class of Novel Point Similarity Measures Based on MAP-MRF Framework for 2D-3D Registation of X-Ray Fluoroscopy to CT Images. , 0, , .		1
214	MATCHING PARAMETERIZED SHAPES BY NONPARAMETRIC BELIEF PROPAGATION. International Journal of Pattern Recognition and Artificial Intelligence, 2009, 23, 209-246.	0.7	1
215	Statistical shape modeling of pathological scoliotic vertebrae: A comparative analysis. , 2010, 2010, 5939-42.		1
216	ECM versus ICP for point registration. , 2011, 2011, 2131-5.		1

ECM versus ICP for point registration. , 2011, 2011, 2131-5. 216

#	Article	IF	CITATIONS
217	Automated 3D Lumbar Intervertebral Disc Segmentation from MRI Data Sets. Lecture Notes in Computational Vision and Biomechanics, 2015, , 131-142.	O.5	1
218	Computer Assisted Planning, Simulation and Navigation of Periacetabular Osteotomy. Lecture Notes in Computer Science, 2016, , 15-26.	1.0	1
219	Atlas-Based Reconstruction of 3D Volumes of a Lower Extremity from 2D Calibrated X-ray Images. Lecture Notes in Computer Science, 2016, , 366-374.	1.0	1
220	Statistical shape modeling of compound musculoskeletal structures around the thigh region. , 2016, ,		1
221	Novel deep learning-based CT synthesis algorithm for MRI-guided PET attenuation correction in brain PET/MR imaging. , 2018, , .		1
222	Statistical Shape Models and Atlases: Application to 2D-3D Reconstruction in THA. , 2018, , 183-190.		1
223	Deep Volumetric Shape Learning for Semantic Segmentation of the Hip Joint from 3D MR Images. Lecture Notes in Computer Science, 2019, , 35-48.	1.0	1
224	DeepASDM: a Deep Learning Framework for Affine and Deformable Image Registration Incorporating a Statistical Deformation Model. , 2021, , .		1
225	Disentangled Representation Learning For Deep MR To CT Synthesis Using Unpaired Data. , 2021, , .		1
226	Non-rigid Free-Form 2D-3D Registration Using Statistical Deformation Model. Lecture Notes in Computer Science, 2015, , 102-109.	1.0	1
227	Fully Automatic X-Ray Image Segmentation via Joint Estimation of Image Displacements. Lecture Notes in Computer Science, 2013, 16, 227-234.	1.0	1
228	Automatic Pose Recovery of the Distal Locking Holes from Single Calibrated Fluoroscopic Image for Computer-Assisted Intramedullary Nailing of Femoral Shaft Fractures. Lecture Notes in Computer Science, 2006, , 195-202.	1.0	1
229	Advanced Technologies in Navigation. , 2007, , 582-585.		1
230	PS-GANS: A Patient-Specific, Gravity Assisted Navigation System for Acetabular Cup Placement. Lecture Notes in Computer Science, 2011, , 101-112.	1.0	1
231	A Cost-Effective Surgical Navigation Solution for Periacetabular Osteotomy (PAO) Surgery. Lecture Notes in Computational Vision and Biomechanics, 2016, , 333-348.	0.5	1
232	Augmented Marker Tracking for Peri-acetabular Osteotomy Surgery: A Cadaver Study. , 0, , .		1
233	Zero-dose fluoroscopy-based close reduction and osteosynthesis of diaphyseal fracture of femurs. Studies in Health Technology and Informatics, 2006, 119, 592-4.	0.2	1
234	Accurate and reliable pose recovery of distal locking holes in computer-assisted intra-medullary nailing of femoral shaft fractures: A preliminary study. Computer Aided Surgery, 2007, 12, 138-151.	1.8	1

#	Article	IF	CITATIONS
235	Deep Learning based Segmentation of Lumbar Vertebrae from CT Images. , 0, , .		1
236	Projector-Based Augmented Reality System for Computer Assisted Orthopaedic Surgery. , 0, , .		1
237	Multi-resolution elastic registration of CT and MR brain images. , 0, , .		0
238	Reconstruction of surfaces from contour data based on recursive medial axis of morphology-difference image and marching contour algorithm. , 0, , .		0
239	RANSAC-based EM algorithm for robust detection and segmentation of cylindrical fragments from calibrated C-arm images. , 2006, , .		Ο
240	An optimal three-stage method for anatomical shape reconstruction from sparse information using a dense surface point distribution model. , 2006, , .		0
241	A Computational Framework for Automatic Determination of Morphological Parameters of Proximal Femur from Intraoperative Fluoroscopic Images. , 2006, , .		0
242	Determining Geometrical Parameters by Particle Filter for Automatic Reconstruction of Surface Model of Proximal Femur from Biplanar Calibrated Fluoroscopic Images. , 2006, , .		0
243	PRECISE POSE RECOVERY OF DISTAL LOCKING HOLES FROM SINGLE CALIBRATED FLUOROSCOPIC IMAGE VIA A NOVEL VARIABLE DECOMPOSITION APPROACH. , 2007, , .		Ο
244	Hardware accelerated ray cast of volume data and volume gradient for an optimized splines-based multi-resolution 2D-3D registration. , 2007, , .		0
245	Robust automatic detection and removal of fiducial projections in fluoroscopy images: An integrated solution. , 2008, 2008, 78-81.		Ο
246	Robust intensity-based 3D-2D registration of ct and X-ray images for precise estimation of cup alignment after total hip arthroplasty. , 2008, , .		0
247	An Integrated Approach for Reconstructing a Surface Model of the Proximal Femur from Sparse Input Data and a Multi-Level Point Distribution Model. Lecture Notes in Computer Science, 2008, , 59-68.	1.0	0
248	Automatic extraction of proximal femur contours from calibrated X-ray images: a Bayesian inference approach. International Journal of Functional Informatics and Personalised Medicine, 2009, 2, 231.	0.4	0
249	Kernel density correlation based non-rigid point set matching for statistical model-based 2D/3D reconstruction. , 2011, , .		0
250	Fully Automatic Segmentation of Hip CT Images via Random Forest Regression-Based Atlas Selection and Optimal Graph Search-Based Surface Detection. Lecture Notes in Computer Science, 2015, , 640-654.	1.0	0
251	Gravity-Assisted Navigation System for Total Hip Arthroplasty. Advances in Experimental Medicine and Biology, 2018, 1093, 181-191.	0.8	0
252	Guest Editorial Multi-Modal Computing for Biomedical Intelligence Systems. IEEE Journal of Biomedical and Health Informatics, 2021, 25, 3256-3257.	3.9	0

#	Article	IF	CITATIONS
253	A CT-Free Intraoperative Planning and Navigation System for High Tibial Dome Osteotomy. Lecture Notes in Computer Science, 2004, , 610-620.	1.0	0
254	Finding Deformable Shapes by Point Set Matching Through Nonparametric Belief Propagation. Lecture Notes in Computer Science, 2006, , 60-67.	1.0	0
255	New CAS Techniques in Trauma Surgery. , 2007, , 496-500.		0
256	An Integrated Approach for Reconstructing Surface Models of the Proximal Femur from Sparse Input Data for Surgical Navigation. Lecture Notes in Computer Science, 2007, , 767-775.	1.0	0
257	Non-photorealistic rendering of virtual implant models for computer-assisted fluoroscopy-based surgical procedures. , 2007, , .		0
258	Automatic Mutual Nonrigid Registration of Dense Surfaces by Graphical Model Based Inference. Lecture Notes in Computer Science, 2008, , 694-704.	1.0	0
259	A Hierarchical Strategy for Reconstruction of 3D Acetabular Surface Models from 2D Calibrated X-Ray Images. Lecture Notes in Computer Science, 2012, , 74-83.	1.0	Ο
260	Robust Proximal Femur Segmentation in Conventional X-Ray Images via Random Forest Regression on Multi-resolution Gradient Features. Lecture Notes in Computer Science, 2013, , 442-450.	1.0	0
261	Image-Guided Orthopaedic Surgery. , 2014, , 647-659.		Ο
262	Fully Automatic CT Segmentation for Computer-Assisted Pre-operative Planning of Hip Arthroscopy. Lecture Notes in Computer Science, 2014, , 55-63.	1.0	0
263	Preoperative Planning of Periacetabular Osteotomy (PAO). Lecture Notes in Computational Vision and Biomechanics, 2016, , 151-171.	0.5	Ο
264	Localization and Segmentation of 3D Intervertebral Discs from MR Images via a Learning Based Method: A Validation Framework. Lecture Notes in Computer Science, 2016, , 141-149.	1.0	0
265	Atlas-Based 3D Intensity Volume Reconstruction of Musculoskeletal Structures in the Lower Extremity from 2D Calibrated X-Ray Images. Lecture Notes in Computer Science, 2017, , 35-43.	1.0	Ο
266	Affinely Registered Multi-object Atlases as Shape Prior for Grid Cut Segmentation of Lumbar Vertebrae from CT Images. Lecture Notes in Computer Science, 2018, , 90-95.	1.0	0
267	Incorporating Spatial Information into 3D-2D Image Registration. Lecture Notes in Computer Science, 2007, , 792-800.	1.0	Ο
268	Unifying Energy Minimization and Mutual Information Maximization for Robust 2D/3D Registration of X-Ray and CT Images. , 2007, , 547-557.		0
269	Graphical User Interface for Joint Space Width Assessment by Optical Marker Tracking. , 2021, , .		0
270	Fully Automatic Segmentation and Landmarking of Hip CT Images. , 0, , .		0

271 3XPlan: A Novel Technology for 3D Prosthesis Planning Using 2D X-ray Radiographs. , 0, , . 0	#	Article	IF	CITATIONS
	271	3XPlan: A Novel Technology for 3D Prosthesis Planning Using 2D X-ray Radiographs. , 0, , .		0